



HAL
open science

Thermodynamic Effects on Grade Transition of Polyethylene Polymerization in Fluidized Bed Reactors

Sabrine Kardous, Timothy Mckenna, Nida Sheibat-Othman

► **To cite this version:**

Sabrine Kardous, Timothy Mckenna, Nida Sheibat-Othman. Thermodynamic Effects on Grade Transition of Polyethylene Polymerization in Fluidized Bed Reactors. *Macromolecular Reaction Engineering*, 2020, 14 (4), pp.2000013. 10.1002/mren.202000013 . hal-02749293v3

HAL Id: hal-02749293

<https://hal.science/hal-02749293v3>

Submitted on 15 Apr 2021

HAL is a multi-disciplinary open access archive for the deposit and dissemination of scientific research documents, whether they are published or not. The documents may come from teaching and research institutions in France or abroad, or from public or private research centers.

L'archive ouverte pluridisciplinaire **HAL**, est destinée au dépôt et à la diffusion de documents scientifiques de niveau recherche, publiés ou non, émanant des établissements d'enseignement et de recherche français ou étrangers, des laboratoires publics ou privés.

Thermodynamic effects on grade transition of polyethylene polymerization in fluidized bed reactors

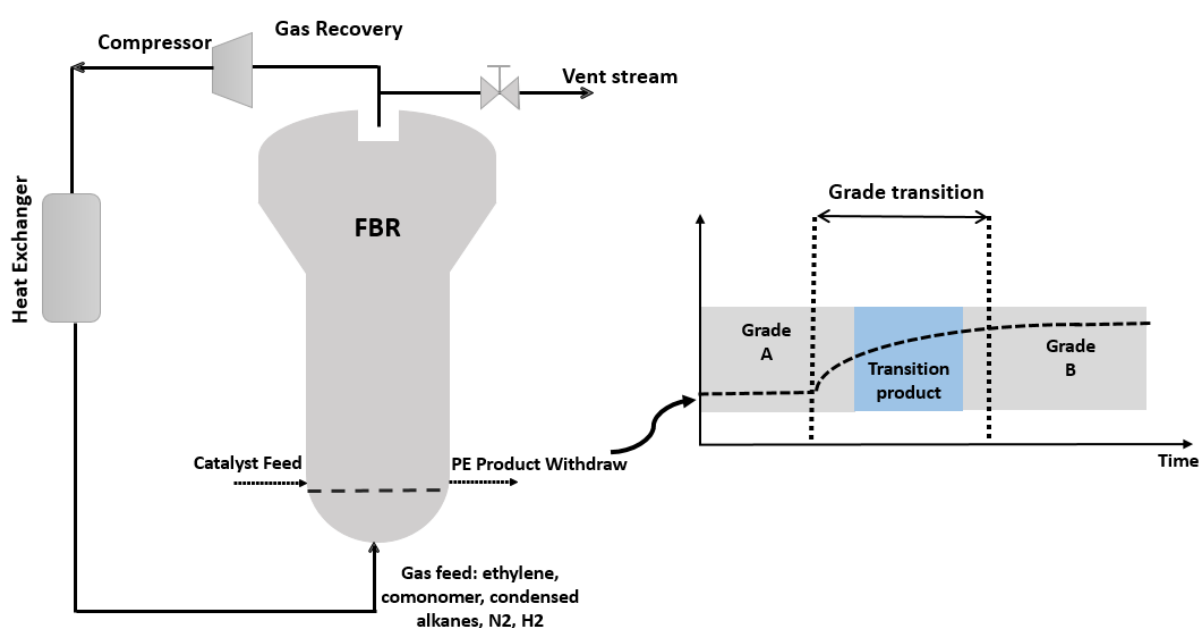
Sabrine Kardous¹, Timothy F.L. McKenna², Nida Sheibat-Othman^{1*}

¹ Université of Lyon, Université Claude Bernard Lyon 1, CNRS, UMR 5007, LAGEPP, F-69100, Villeurbanne, France

² Université of Lyon, Université Claude Bernard Lyon 1, CPE Lyon, CNRS, UMR 5265, C2P2 - LCPP group, Villeurbanne, France.

*E-mail : nida.othman@univ-lyon1.fr

Graphical abstract



Abstract

An off-line dynamic optimization procedure is employed to optimize the transition between different grades of linear low density polyethylene in a fluidized-bed reactor. This type of reactor is frequently operated under condensed mode, which consists of injecting induced

condensing agents (ICA) to absorb part of the reaction heat. However, the presence of ICA affects the solubility of monomers in the polymer, so it is important to account for this effect in a grade transition optimization strategy. A kinetic model is combined with a thermodynamic model based on the Sanchez-Lacombe equation of state to describe the grade transitions. Simplified correlations are then suggested to predict the impact of ICA on ethylene and comonomer solubility in a quaternary system. The results highlight the importance of the thermodynamic model during grade transition.

Keywords

Grade transition, fluidized bed reactor, condensed mode cooling, thermodynamics, polyethylene.

1. Introduction

Polyethylene (PE) is the most widely produced polymer in the world. Among the different types of PE, linear low density polyethylene (LLDPE) occupies an important position with around 30% of the global PE production in 2018.^[1] Most processes used to make LLDPE are gas-phase processes which provide several advantages over slurry processes. Indeed, difficulties related to mass transfer limitations and the dissolution of the amorphous polymer in a diluent, as well as fouling in slurry processes are avoided in gas-phase processes. Gas-phase processes are adequate for multipurpose production and permit the production of a wide range of PE grades. Among gas-phase processes, fluidized-bed reactors (FBRs) are far and away the most widely used reactors for the production of LLDPE because they are the only reactors that can remove enough heat in the gas phase and thus allow the production of large amounts of polymer.^[2] In order to further enhance heat transfer and increase productivity, condensed mode cooling is frequently employed, where induced condensed agents (ICAs), which are typically alkanes such

propane or isomers of butane, pentane or hexane, are injected in either liquid or vapor form.^[3,4] The heat of vaporization and/or increase in the heat capacity of the vapor phase in the reactor absorb a significant amount of the reaction heat and improve the control of the reactor temperature. However, it has also been observed that when the polymer particles are swollen by an alkane or an alkene, the reaction rate can change significantly due to the so-called cosolubility effect. Indeed, the presence of a hydrocarbon heavier than ethylene enhances the solubility of the latter in the amorphous phase of the polymer, thereby contributing to a higher rate of polymerization, while the lighter hydrocarbons play the role of anti-solvent for the heavier ones.^[5,6] Therefore, the presence of ICA increases the ethylene concentration in the particles, leading to a higher reaction rate, while ethylene is expected to act as an anti-solvent for the ICAs (and eventually for comonomers like 1-butene or 1-hexene). This is expected to impact the properties of the final product such as its molecular weight and density. Therefore, it is important to account for these effects in the process model, especially in model-based optimization or control strategies.

It is quite common to produce several grades in the same polymerization plant in order to obtain a PE with different density, molecular weight and polydispersity index required in the various applications of PE.^[7] Frequent transitions between these grades are usually needed to suit the market demand and reduce the storage cost. Due to the long residence time in FBRs, compared to tubular or loop reactors for instance, the flow rates should be optimized wisely to ensure attaining the new set-point in a short time, thus reducing the amount of transition product. When condensed mode is employed, the transitions might be more complex since the sorption/desorption dynamics of the different species can change the behavior of the system. The employment of an adapted control of the transition is thus essential in order to optimize the economic yield while ensuring the security of the operations.

Debling et al.^[7] studied the effect of different parameters on grade transition of solution, slurry, bulk and gas-phase polyolefin reactions in commonly used reactors, including horizontal or vertical stirred beds, loop and FBRs. They indicated the residence time distribution of the different components to be a determining factor in the speed of grade transition and summarized the procedures employed to speed the transition in FBRs, such as de-inventorying the reactor content or venting/overshooting the gases at the beginning of the transition. However, they did not investigate the effect of ICA on the residence time of the reactor. Rahimpour et al.^[8] also indicated that partial venting of the reactor, composing a new gas phase and reducing the bed level reduce the quantity of transition product in PE FBRs. They highlighted that such so-called *semi-continuous* strategy was necessary in some situations in order to keep the reactor temperature between the gas dew point and the polymer melting point (to avoid agglomeration of the particles), which could not be achieved with the continuous strategy (i.e. by controlling only the flow rates). Note that the flow rates employed during the transition were those used for the final grade, which were calculated by solving the model equations under steady state conditions, and identifying the boundary conditions to be implemented for each new grade. However, numerous works indicated that the flow rates of the final grade do not necessarily ensure the best transition, and suggested the employment of dynamic optimization or control algorithms to ensure better transitions.^[9,10]

For the particular problem of grade transition in FBRs, most works are based on offline optimization due to the long calculation time and the complexity of problem formulation. McAuley et al.^[11,12] were the first to investigate dynamic optimization of grade transition of PE in gas-phase FBR. They provided a kinetic model for copolymerization, correlations for the final properties based on patent data (i.e. melt index and polymer density), and modelled the FBR as a continuous stirred tank reactor (CSTR) due to its high recycle ratio and low single pass conversion. The suggested control variables were the flow rates of hydrogen and

comonomer (1-butene or 1-hexene), as they directly affect the polymer molecular weight and density. Afterwards, optimization strategies were proposed for different types of processes, for instance for slurry high density polyethylene (HDPE) processes composed of two loop reactors^[13] or two CSTRs.^[14]

Furthermore, different improvements in the optimization approaches were suggested. For instance, Chatzidoukas et al.^[15] proposed a mixed integer dynamic optimization approach to realize a closed-loop control in a fluidized-bed reactor. Nystrom et al.^[16] employed a comparable approach based on dynamic optimization combined to a mixed-integer linear problem related to the sequencing, and solved these decoupled problems by iteration. Bonvin et al.^[17] proposed to employ a measurement-based approach by tracking the necessary conditions of optimality, for instance based on run-to-run basis, in order to correct for modelling mismatch in a homopolymerization process.

Regarding closed-loop control, it was usually considered using algorithms based on an optimization criterion, such as model predictive control (MPC). The closed-loop character of MPC makes it more robust to modelling errors than open-loop dynamic optimization. But, in order to allow its online implementation in FBRs, part of the optimization is usually solved offline. For instance, Wang et al.^[18] combined an offline optimizer and a nonlinear MPC, where the optimal feed rates were calculated offline and the MPC allowed minimizing the modeling error and updating the feed rates. A shrinking horizon nonlinear model predictive control with expanding horizon least-squares estimation was also implemented to control the grade transition in FBRs.^[19]

Among all the cited works, in terms of methodology, dynamic optimization-based policies were the most widely used for gas-phase processes, and they will therefore be employed in this work. Indeed, the optimization criterion is more flexible and can be tuned to optimize instantaneous or cumulative properties during transition, or the transition time. In addition, the previous

literature analysis highlights that the parameters that most affect the grade transition are the residence time (distribution) and the hydrogen and comonomer flow rates. However, the thermodynamic interactions that are due to the use of a condensing agent and/or comonomer were not considered. This work is focused particularly on condensed mode, and will explore the implications of using a more representative thermodynamic model than most works that takes into account the interactions between the different species. It is clear that simply using additive solubilities will lead to erroneous conclusions about reaction rates and product properties. It is thus important to understand whether or not this is an important part in optimizing grade transitions.

In this work, the grade transition of PE copolymers in a gas-phase FBR operating under condensed mode is considered. First the effect of ICA (n-hexane or iso-butane) on the absorption of monomer (ethylene) and comonomer (1-butene or 1-hexene) is investigated using a model based on the Sanchez-Lacombe equation of state (SL EOS) and experimental data from literature.^[20,21] Since no sufficient experimental data are available in the open literature for quaternary systems (i.e. a copolymerization in presence of an ICA), simplifying correlations are proposed in order to allow for fast prediction of the co-solubility effects in a quaternary system.^[21] The thermodynamic correlations are then used to calculate equilibrium solubilities for two copolymerization systems of ethylene with α -olefins. The thermodynamic predictions are combined with kinetic copolymerization models to model the dynamic behavior of the FBR, which is assumed to behave like a single-phase CSTR. The model is valid in the super-dry upper compartment of the FBR, containing only gas and polymer. This dynamic model is finally used within a dynamic optimization strategy to optimize the transitions between different grades of LLDPE.

2. Gas-phase catalytic ethylene co-polymerization model

2.1 Thermodynamic model

The SL EOS has been used frequently to predict the thermodynamic behavior in binary and ternary systems (polymer plus one or two penetrants respectively).^[22,23] However, as discussed by McKenna^[3], solubility data for systems of two penetrants is very scarce, and realistic data for multiple penetrants is totally absent from the open literature. Therefore, in the absence of a reliable data set, we will propose a simplified model accounting for 3 penetrants (i.e. quaternary system) in an LLDPE plant. Two systems are considered, at 90°C, which are frequently employed in industry:

1. Copolymerization of ethylene and 1-hexene in presence of n-hexane as ICA
2. Copolymerization of ethylene and 1-butene in presence of iso-butane as ICA

In the Sanchez-Lacombe EOS, the concentration of the different components in the polymer is predicted based on the binary interaction parameters (k_{ij}) between each pair of components (the penetrating species and the polymer). The thermodynamic model is based on the following assumptions: i) The gases dissolve only in the amorphous phase^[24]; ii) The interaction between molecules of olefins and/or ICA is ideal.^[25] Thus, in a quaternary system of three penetrating gaseous species, ethylene (1), ICA (2) and comonomer (3), in the polymer (4), k_{12} , k_{13} and k_{23} are equal to zero. Finally, only the global degree of crystallinity of the polymer is accounted for in the thermodynamic model. Strictly speaking, also tie molecules linking the crystalline lamellae can influence the solubility of different species in the amorphous phase.^[26]

Due to the lack of solubility data, the following, more critical assumptions are considered:

A.1 *Additive effect*: The quaternary system is approximated by a ternary system: ethylene/ (ICA+comonomer)/ LLDPE, as suggested by Alves et al.^[21] Thus, a “pseudo” component, representing the mixture of ICA plus comonomer, is defined for which the thermodynamic

parameters are identified. In this assumption, no interaction between ICA and comonomer is considered, which means that these species behave independently from each other as if they were present in a ternary system (PE, ethylene and either ICA or comonomer). This is not unreasonable if the comonomer and ICA are similar in structure. This assumption is thus applicable for the two systems studied in this work, i.e the comonomer 1-hexene and n-hexane as ICA, as well as the comonomer 1-butene and iso-butane as ICA. However, this assumption does not mean that the ICA and the comonomer have the same solubility or co-solubility effect, as discussed in the following two sections.

A2. Polynomial approximations: In order to reduce the computation time, the results from the SL EOS or the experimental results, are approximated by polynomials of degree 1 or 2, as suggested by Alves et al.^[21] Different pathways were considered for the two systems investigated in the present work, as described in the following sections.

2.1.1 Polyethylene, in presence of ethylene, 1-hexene and the ICA n-hexane

For the first system, the comonomer 1-hexene and the ICA n-hexane, both the comonomer and the ICA were found to have comparable solubilities in a binary system, especially at low pressure, as shown by Figure 1 (Yao et al.^[27] and Jin et al.^[28]). Therefore, Alizadeh et al.^[23] assumed it safe to consider that they have similar solubility in LLDPE in a ternary or quaternary system. A similar observation was found for other 3 and 6 carbon pairs, such as the isomers propene and propane, where the difference in their solubility constant of Henry's law was 10% at 25°C, as reported by Michaels et al.^[24]. This can be explained by the fact that 1-hexene and n-hexane have similar shapes and same number of carbons, so almost the same size, therefore, they have similar tendency to condense (i.e., same volatility). Besides, they have similar nature of interaction with LLDPE segments (i.e., same nature of van der Waals forces).^[23] Therefore, in a quaternary system, the ratio of solubility of 1-hexene in LLDPE to n-hexane is assumed

$r = \frac{S_{1\text{-hexene}}}{S_{n\text{-hexane}}} = 1$. Note that for the second system, the comonomer 1-butene and the ICA iso-

butane, their binary solubilities in LLDPE are different, and was accounted for as explained in section 2.1.2.

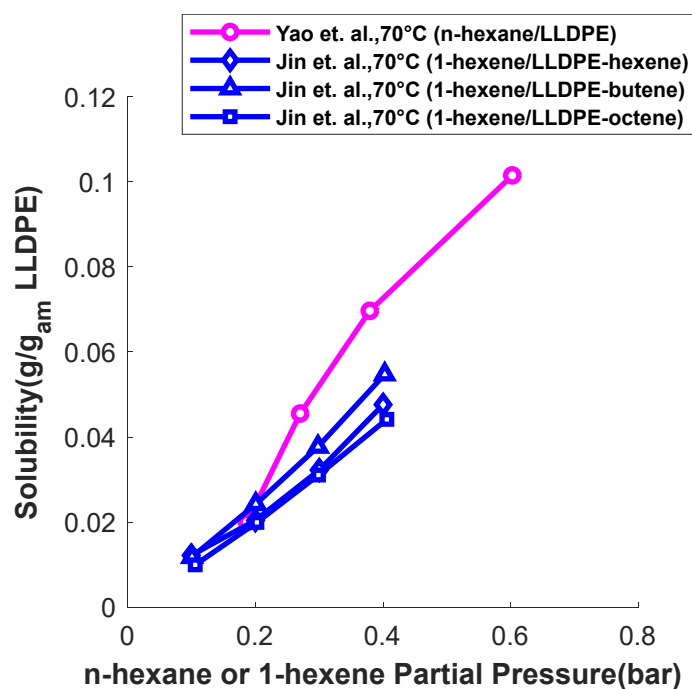


Figure 1. Solubility of n-hexane and 1-hexene in LLDPE (binary systems) at 70°C (data from Yao et al.^[27] and Jin et al.^[28])

For this system, copolymerization of ethylene with 1-hexene in presence of the ICA n-hexane, solubility data are available only for the ternary system ethylene/n-hexane/PE at 10 bar ethylene^[27] (Figure 2). To use these data in a quaternary system (Assumption A1: *Additive effect*), the ICA n-hexane is assumed to thermodynamically behave like the comonomer 1-hexene (as explained in the previous section).^[23]

The available ternary data of solubility (Figure 2) is then used to obtain linear or polynomial equations (Assumption A2: *Polynomial approximations*). It can be noticed that the solubility of ethylene varies linearly over a small range with the pressure of ICA/comonomer, therefore a polynomial of degree 1 could fit the experimental data, while the solubility of comonomer varies nonlinearly with its pressure, therefore a polynomial of degree 2 was necessary, as follows:

$$[M_1^p] = A(P_{ICA} + P_2) + B \quad (1)$$

$$[M_2^p] = r \frac{P_2}{P_2 + P_{ICA}} [C(P_{ICA} + P_2)^2 + D(P_{ICA} + P_2)] \quad (2)$$

Where $[M_i^p]$ and P_i are respectively the concentration in amorphous polymer (mol m^{-3}) and pressure (bar) of component i (1 for ethylene and 2 for the comonomer) and r represents the ratio of solubility of comonomer to ICA, which is equal to one in this system. The values of the coefficients (A, B, C, D) in equations 1 and 2 are given in Table 1. **As the reaction takes place in the amorphous region only, the concentration of monomers in the amorphous phase is used to calculate the reaction rate.** It is important to mention that these coefficients are valid for the specific conditions (temperature and pressure) for which they were developed (i.e. ethylene pressure of 10 bars and pseudo-component ‘ICA+comonomer’ pressure of 0 to 1 bar). It is also important to note that the concentration of ethylene only varies slightly as a function of the partial pressure of “n-hexane +1-hexene”, however the concentration of n-hexane (and so of 1-hexene) is very sensitive to the partial pressure of the pseudo-component ‘ICA+comonomer’, which is necessary to account for in the model (Figure 2). Note that when increasing temperature, the slope of the concentration of n-hexane with its partial pressure decreases (from $C \sim 624$ to $506 \text{ mol m}^{-3} \text{ Pa}^{-2}$), while the slope of the concentration of ethylene increases (from $A \sim 34$ to $279 \text{ mol m}^{-3} \text{ Pa}^{-1}$). Increasing the temperature thus increases slightly the impact of ICA on ethylene absorption, but it remains very low. Besides, the figure shows that the concentration of n-hexane in amorphous PE increases slightly in a binary system compared to a ternary system. This was expected given the anti-solvent effect of ethylene on ICA in a ternary system.^[29,30] Note that the concentration plots presented in this paper were calculated by converting solubility data (in g g^{-1} amorphous polymer) found in the open literature into mol m^{-3} using the amorphous polymer densities (i.e., the values of the swollen polymer density with different ICAs) estimated by Sanchez-Lacombe EoS for each case.

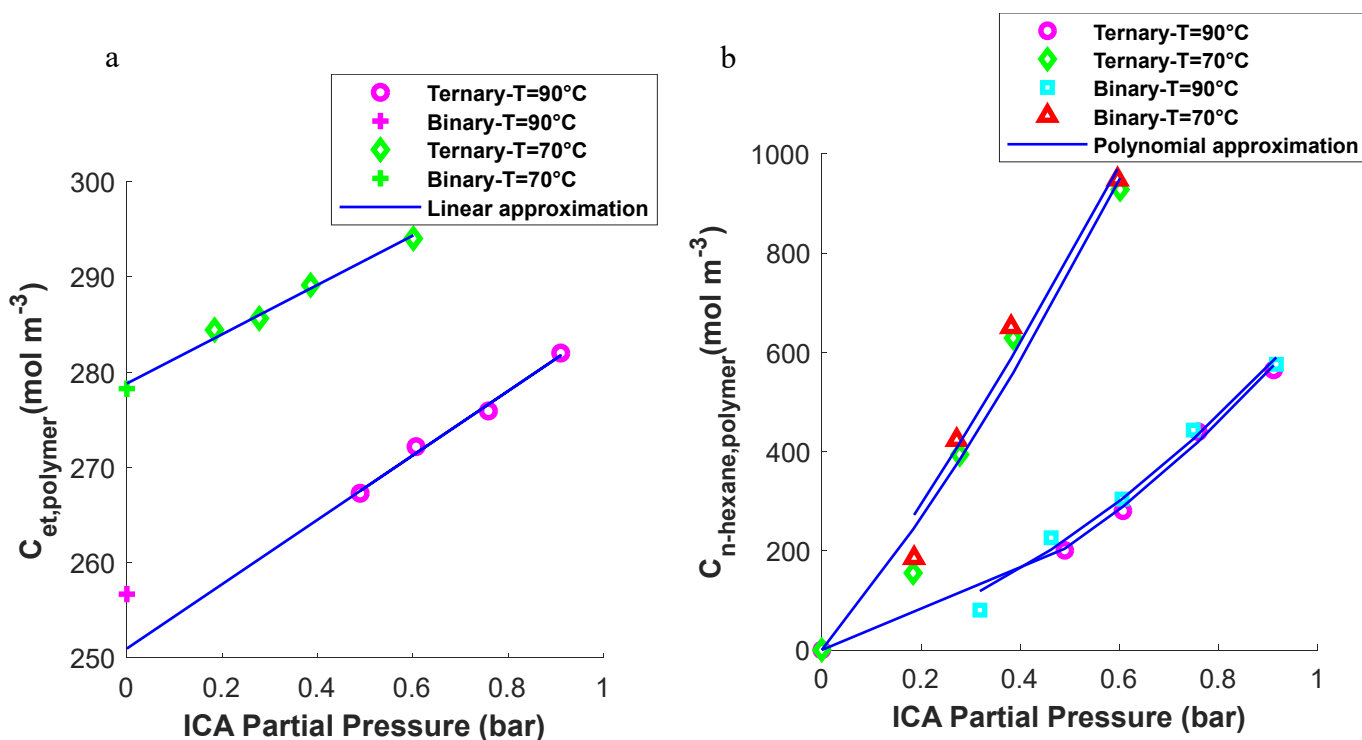


Figure 2. Ternary solubility data ethylene/n-hexane/LLDPE at 90°C and 70°C at 10 bar of ethylene (experimental data are taken for ternary systems from Yao et al.^[31] and for binary systems from Yao et al.^[27]): a) Concentration of ethylene in amorphous LLDPE as a function of the partial pressure of n-hexane, b) Concentration of n-hexane as a function of its partial pressure.

Table 1. Coefficients of the correlations allowing to estimate the ethylene and 1-hexene concentrations in amorphous LLDPE at 90 °C and 70 °C (valid at ethylene pressure of 10 bar and pseudo-component pressure on the range 0-1 bar)

	Value at	Value at	units
	90°C	70°C	
A	33.8	25.9	mol m ⁻³ bar ⁻¹
B	251	278.8	mol m ⁻³
C	505.8	623.9	mol m ⁻³ bar ⁻²
D	169.2	1206.3	mol m ⁻³ bar ⁻¹
r	1	1	-

Equations 1 and 2, with their identified parameters in Table 1, allow for the estimation of the concentration of ethylene and 1-hexene in the quaternary system ethylene/1-hexene/n-

hexane/LLDPE at equilibrium. This information is all what is required for the rest of the paper regarding this system, and there is no need for the SL EoS here.

2.1.2 Polyethylene, in presence of ethylene, 1-butene and iso-butane as ICA

For the copolymerization of ethylene with 1-butene in presence of iso-butane as ICA, ternary data is not available for either ethylene/iso-butane/LLDPE or for ethylene/1-butene/LLDPE. Moreover, the available binary sorption data (Figure 3) ^[32,33] indicates that 1-butene and iso-butane have different solubilities in the polymer and cannot be assumed to be similar, as could be done for 1-butene/n-butane and 1-hexene/n-hexane. Indeed, the solubility of 1-butene in HDPE is higher than that of iso-butane by almost a factor of $r = \frac{S_{1-butene}}{S_{iso-butane}} = 1.78$, at nearly the same temperature.

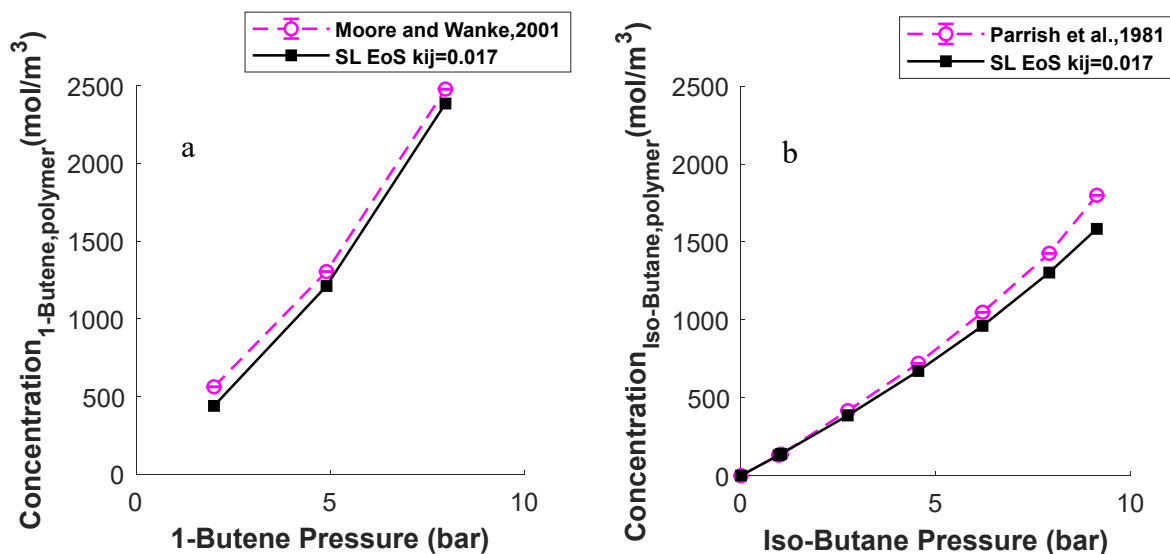


Figure 3. Binary solubility data in HDPE of a) comonomer 1-butene at 68.9°C, and b) ICA iso-butane at 65.6°C.

Due to this lack of data, the following assumptions are made only for this system:

A3. The ratio of sorption of 1-butene to iso-butane, r (Figure 3), identified in a binary system, was assumed to remain unchanged in a ternary system, and to remain unchanged within a

temperature range of 65-90 °C. This means that they are assumed to have the same co-solubility effect on ethylene.

- A4. The k_{ij} parameters are assumed to vary linearly with temperature. So, as solubility data is not available, an extrapolation of k_{ij} is done to predict them at 90°C.
- A5. The solubility of iso-butane in HDPE and LLDPE is assumed to be the same, as only solubility data in HDPE is available (in a binary system^[32]).

Again, Assumption A1 is applied to this system: The comonomer and ICA were assumed to have an additive effect in a quaternary system. Alves et al.^[21] validated this assumption for propane and iso-butane based on reaction data from patents. This means that propane and iso-butane do not affect the solubility of each other (i.e. there is no co-solubility effect), which is reasonable in view of their similarities. A similar assumption can be done regarding 1-butene and iso-butane in our system. Based on this assumption, Alves et al.^[21] estimated the binary interaction parameters k_{ij} for the ternary system ethylene/iso-butane/LLDPE by fitting to experimental solubility data of the binary systems ethylene/LLDPE and iso-butane/HDPE at 70°C (Table 2).^[32] Thus, the correlation between the ICA and the comonomer becomes (combining Assumptions A1, A2 and A3):

$$[M_2^P] = r \frac{P_2}{P_2 + P_{ICA}} E(P_{ICA} + P_2) \quad (3)$$

In order to identify the parameters of equations 1 and 3 for the quaternary system, SL EOS is first used in the ternary system ethylene/iso-butane/LLDPE (with k_{ij} identified using binary solubility data^[21]) to identify the solubility of ethylene and iso-butane at different pressures of iso-butane. Then, the k_{ij} parameters were extrapolated over temperature to have values at 90°C (Assumption A4) (Figure 4, Table 3). The concentration of 1-butene is then calculated using

$S_{1\text{-butene}} = r S_{\text{iso-butane}}$. From the obtained data points, polynomials of order 1 were identified for both ternary systems.

As in the first system, it can be noted that the concentration of ethylene only varies slightly as a function of the partial pressure of the pseudo-component “isobutane+1-butene”, while the concentration of comonomer 1-butene is very sensitive to its partial pressure (Figure 4).

Table 2. Binary interaction parameters of the ternary system ethylene/iso-butane/LLDPE (based on binary thermodynamic data)

Temperature (°C)	Ethylene/iso-butane (k_{12})	Ethylene/LLDPE (k_{13}) [23]	Iso-butane/LLDPE (k_{23})
70°C	0	-0.014	0.025 (74°C) [21]
80°C	0	-0.022	0.022 (82°C) [21]
90°C	0	-0.032	$-3.75 \cdot 10^{-4} T(\text{K}) + 0.1551$

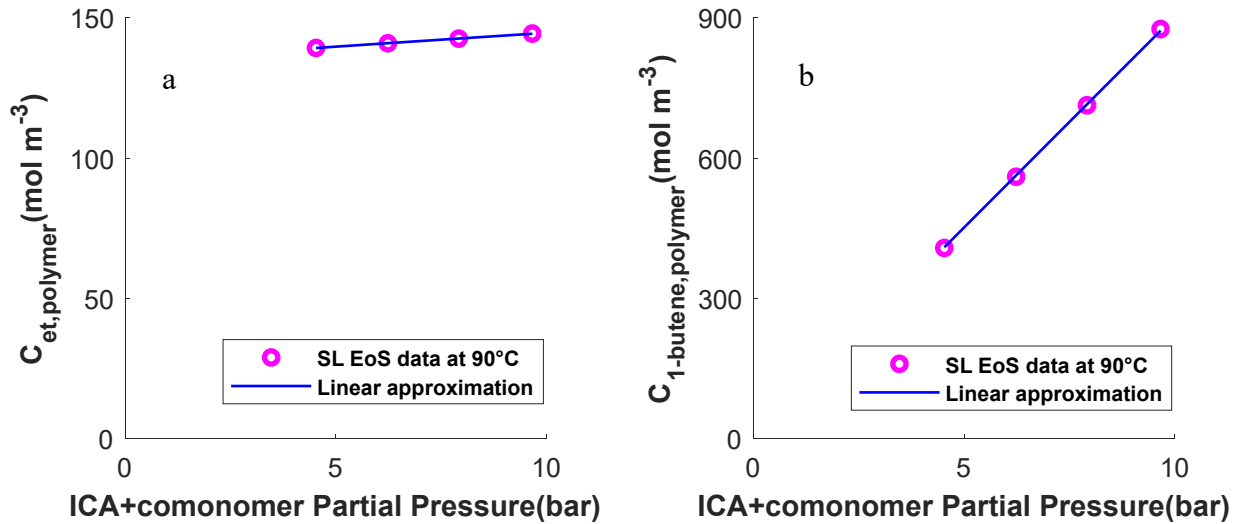


Figure 4. Concentrations in amorphous LLDPE obtained using SL EoS, Pseudo-quaternary system ethylene/(ICA+comonomer)/HDPE, at 90°C (after extrapolation of k_{ij}) and 7 bar of ethylene: a) ethylene and b) comonomer 1-butene.

Table 3. Coefficients of the correlations allowing to estimate the ethylene and 1-butene concentrations in amorphous LLDPE at 90°C (valid at ethylene pressure of 7 bar and pseudo-component pressure on the range 5-10 bar)

Parameter	at 90°C	Units
<i>A</i>	0.992	mol m ⁻³ Pa ⁻¹
<i>B</i>	134.73	mol m ⁻³
<i>E</i>	90.209	mol m ⁻³ Pa ⁻¹
<i>r</i>	1.78	-

2.2 Kinetic model

A classical reaction scheme (Table 4) of copolymerization of ethylene in presence of a catalyst having one type of active sites was considered (see for instance de Carvalho et al.^[34], McAuley et al.^[35], Chatzidoukas et al.^[15]). The only difference between the two copolymerization systems, with the comonomer 1-hexene or with 1-butene, is the values of the rate constants.

The following notations are used in Table 4: S_p : potential catalyst active sites, P_0 : activated vacant catalyst sites, P_* : total active sites (vacant P_0 and occupied by a polymer chain $P_{n,i}$), $P_{n,i}$: living copolymer chains of length n ending with monomer i , D_n : dead copolymer chains of length n and C_d : deactivated catalyst sites.

The reaction rates resulting from the proposed reaction scheme are given in Table 5. All concentrations are in (mol m⁻³) and the following notations are used: λ_k moment k of living chains, μ_k moment k of dead chains and $M_{w,c}$ is the **cumulative** polymer average molecular weight.

Table 4. Kinetic scheme of the copolymerization of ethylene with a catalyst of one site (without co-catalyst)

Designation	Reaction
Spontaneous activation	$S_p \xrightarrow{k_a} P_0$
Chain initiation	$P_0 + M_i \xrightarrow{k_{oi}} P_{1,i}$
Propagation	$P_{n,i} + M_j \xrightarrow{k_{pij}} P_{n+1,j}$

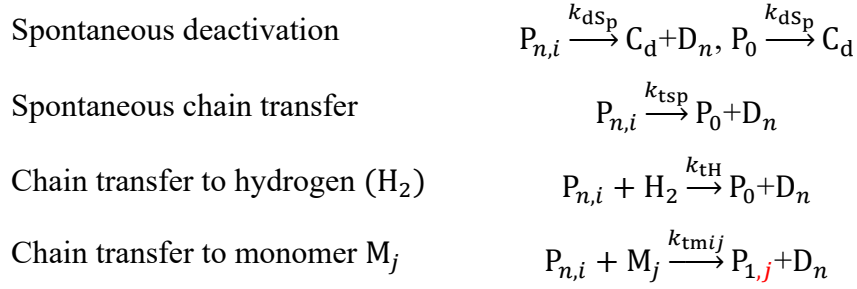


Table 5. Reaction rates of the different species (mol m⁻³ s⁻¹)

$R_{Sp} = -k_a[S_p]$
$R_{P_0} = k_a[S_p] - k_{dSp}[P_0] - (k_{01}[M_1^P] + k_{02}[M_2^P])[P_0] + (k_{tSp} + k_{tH}[H_2^P])\lambda_0$
$R_{\lambda_0} = [P_0](k_{01}[M_1^P] + k_{02}[M_2^P]) - \lambda_0 (k_{dSp} + k_{tSp} + k_{tH}[H_2^P])$
$R_{\lambda_1} = [P_0](k_{01}[M_1^P] + k_{02}[M_2^P]) + \lambda_0 ((k_{tm11}\phi_1 + k_{tm21}\phi_2 + k_{p11}\phi_1 + k_{p21}\phi_2)[M_1^P] + (k_{tm12}\phi_1 + k_{tm22}\phi_2 + k_{p12}\phi_1 + k_{p22}\phi_2)[M_2^P]) - \lambda_1 (k_{dSp} + k_{tSp} + k_{tH}[H_2^P] + (k_{tm11}\phi_1 + k_{tm21}\phi_2)[M_1^P] + (k_{tm12}\phi_1 + k_{tm22}\phi_2)[M_2^P])$
$R_{\lambda_2} = [P_0](k_{01}[M_1^P] + k_{02}[M_2^P]) + \lambda_0 ((k_{tm11}\phi_1 + k_{tm21}\phi_2)[M_1^P] + (k_{tm12}\phi_1 + k_{tm22}\phi_2)[M_2^P]) + (\lambda_0 + 2\lambda_1) ((k_{p11}\phi_1 + k_{p21}\phi_2)[M_1^P] + (k_{p12}\phi_1 + k_{p22}\phi_2)[M_2^P]) - \lambda_2 (k_{dSp} + k_{tSp} + k_{tH}[H_2^P] + (k_{tm11}\phi_1 + k_{tm21}\phi_2)[M_1^P] + (k_{tm12}\phi_1 + k_{tm22}\phi_2)[M_2^P])$
$R_{\mu_0} = \lambda_0 (k_{dSp} + k_{tSp} + k_{tH}[H_2^P] + (k_{tm11}\phi_1 + k_{tm21}\phi_2)[M_1^P] + (k_{tm12}\phi_1 + k_{tm22}\phi_2)[M_2^P])$
$R_{\mu_1} = \lambda_1 (k_{dSp} + k_{tSp} + k_{tH}[H_2^P] + (k_{tm11}\phi_1 + k_{tm21}\phi_2)[M_1^P] + (k_{tm12}\phi_1 + k_{tm22}\phi_2)[M_2^P])$
$R_{\mu_2} = \lambda_2 (k_{dSp} + k_{tSp} + k_{tH}[H_2^P] + (k_{tm11}\phi_1 + k_{tm21}\phi_2)[M_1^P] + (k_{tm12}\phi_1 + k_{tm22}\phi_2)[M_2^P])$
$R_{H_2} = k_{tH}[H_2^P]\lambda_0$
$R_{M_1} = (k_{01}[P_0] + (k_{tm11}\phi_1 + k_{tm21}\phi_2 + k_{p11}\phi_1 + k_{p21}\phi_2)\lambda_0)[M_1^P]$
$R_{M_2} = (k_{02}[P_0] + (k_{tm22}\phi_2 + k_{tm12}\phi_1 + k_{p22}\phi_2 + k_{p12}\phi_1)\lambda_0)[M_2^P]$
With $\phi_1 = \frac{k_{p21}[M_1^P]}{k_{p12}[M_2^P] + k_{p21}[M_1^P]}$, $\phi_2 = 1 - \phi_1$,
$[H_2^P]$ (mol m ⁻³ am. polymer) = $S_{H_2} \frac{\rho_{PE}}{MW_{H_2}}$, S_{H_2} (g H ₂ g ⁻¹ am. polymer) = $10^{-9} P_{H_2}$ ^[36]

$$\lambda_k = \lambda_{k,1} + \lambda_{k,2} = \sum_{n=1}^{\infty} n^k [P_{n,1}] + \sum_{n=1}^{\infty} n^k [P_{n,2}],$$

$$\mu_k = \sum_{n=2}^{\infty} n^k [D_n]$$

$$M_{w,i} = M_{w,m} \frac{\lambda_2}{\lambda_1}, M_{w,c} = M_{w,m} \frac{(\lambda_2 + \mu_2)}{(\lambda_1 + \mu_1)}, \text{ with } M_{w,m} = \sum_{i=1}^2 \varphi_i M_{wi}, \varphi_i = \frac{R_{M_i}}{\sum_{i=1}^2 R_{M_i}}$$

The values of the different kinetic rate constants are given in Tables 6 and 7. E refers to the activation energy and k_0 to the pre-exponential factor. For the case of ethylene-*co*-1-butene, the parameters were taken from Chatzidoukas et al.^[15] or Ghasem et al.^[37]. For the system ethylene-*co*-1-hexene in gas-phase, fewer parameters are available. Chakravarti et al.^[38] gave some kinetic parameters for this system using a metallocene catalyst. In order to keep both systems comparable in terms of catalyst activity, only the reactivity ratios were taken from Chakravarti et al.^[38], and the other parameters and ratios were kept as for the first system. The identification of a specific kinetic model for a defined system is out of the scope of this work as our primary focus is to explore the impact of the co-solubility effect on grade change optimization.

Table 6. Pre-exponential factors and activation energies of the kinetic parameters of co-polymerization of ethylene and a comonomer (common values for both systems) ($k_i = k_{i,0} e^{-\frac{E_a}{RT}}$)

Parameter	Value
Spontaneous activation ^[37]	
$k_{a,0}$ (s ⁻¹)	7.2×10^4
E_a (J mol ⁻¹)	33472
Spontaneous deactivation ^[15]	
$k_{dsp,0}$ (s ⁻¹)	7.2
E_{dsp} (J mol ⁻¹)	33472
Initiation ^[37]	
$k_{0,1}$ (m ³ mol ⁻¹ s ⁻¹)	2.9×10^2
$E_{0,1}$ (J mol ⁻¹)	37656
Spontaneous chain transfer ^[15]	
$k_{tsp,0}$ (m ³ mol ⁻¹ s ⁻¹)	7.2
E_{tsp} (J mol ⁻¹)	33472

Transfer to hydrogen ^[37]	
$k_{tH,0}$ (m ³ mol ⁻¹ s ⁻¹)	6.3
E_{tH} (J mol ⁻¹)	33472
Transfer to monomer ^[37]	
$k_{tm11,0}$ (m ³ mol ⁻¹ s ⁻¹)	0.15
$k_{tm12,0}$ (m ³ mol ⁻¹ s ⁻¹)	0.43
$k_{tm21,0}$ (m ³ mol ⁻¹ s ⁻¹)	0.15
$k_{tm22,0}$ (m ³ mol ⁻¹ s ⁻¹)	0.43
$E_{tmij,0}$ (J mol ⁻¹)	33472
Activation energy of propagation ^[15]	
E_{pij} (J mol ⁻¹)	37656

Table 7. Propagation rate coefficients of the co-polymerization of ethylene with a comonomer

	1-Butene	1-Hexene
Reactivity ratios (-):		
$r_1 = k_{p11}/k_{p12}$	42.5	18.94 ^[38]
$r_2 = k_{p22}/k_{p21}$	0.023	0.04 ^[38]
Pre-exponential factor of propagation(m ³ mol ⁻¹ s ⁻¹):		
$k_{p11,0}$	2.48×10^4 ^[37]	2.48×10^4
$k_{p12,0}$	5.82×10^2 ^[37]	$k_{p11}/r_1 = 1.3 \times 10^3$
$k_{p21,0}$	1.86×10^4 ^[37]	$k_{p22}/r_2 = 2.65 \times 10^3$
$k_{p22,0}$	4.37×10^2	1.06×10^2 ^{[38]*}
Comonomer initiation (m ³ mol ⁻¹ s ⁻¹):		
$k_{0,2}$	40.7 ^[37]	$k_{0,1}k_{p22}/k_{p11} = 1.25$
$E_{0,2}$ (J mol ⁻¹)	37656	37656

* Calculated to respect the ratio k_{p11}/k_{p22} in reference^[38].

2.3 Fluidized bed reactor model

The FBR is modeled as a single-phase CSTR. This assumption is a reasonable initial approximation in industrial FBR given its high recycle ratio and low single pass conversion.^[8]

^{35]} Fresh or prepolymerized catalyst particles, gas species (monomers, N₂, H₂) and condensed gas (ICA) are assumed to be fed continuously at the bottom of the reactor. Thus, the FBR can roughly be divided into two compartments: one super-dry compartment in the containing only gas and polymer, and one much smaller compartment in the bottom also containing condensed vapors. Only the upper compartment is considered in the present model, which represents most of the reactor volume. Indeed, when operating under condensed mode, the injected liquid species evaporate rapidly and the major part of the reactor only contains solid and gas species (i.e. super-dry mode).^[39]

The mass balances of the different species in the FBR are given in Table 8, with the following notations, ε_{bed} : porosity of the bed, X_i and $X_{i,in}$: mass fractions of component i in the recycle and the input stream respectively, h (m): bed height, V_{bed} (m³): bed volume, A (m²): cross-sectional area of the bed Q_0 (m³ s⁻¹): bed outlet volumetric flow rate, F_k (kg s⁻¹) inlet flow rate of component k , F_{rec} (kg s⁻¹) recycling flow rate and X_k mass fraction of component k in the gas phase.

Table 8: Mass balances of the different species in the FBR

Monomer i	$\frac{d[M_i]}{dt} = \frac{F_i}{M_{wi}\varepsilon_{bed}V_{bed}} - \frac{Q_0[M]_i}{V_{bed}} - \frac{(1 - \varepsilon_{bed})}{\varepsilon_{bed}} R_{M_i} - \frac{[M]_i A dh}{V_{bed} dt}$
Hydrogen	$\frac{d[H_2]}{dt} = \frac{F_{H_2}}{M_{w,H_2}\varepsilon_{bed}V_{bed}} - \frac{Q_0[H_2]}{V_{bed}} - \frac{(1 - \varepsilon_{bed})}{\varepsilon_{bed}} R_{H_2} - \frac{[H_2] A dh}{V_{bed} dt}$
Nitrogen	$\frac{d[N_2]}{dt} = \frac{F_{N_2}}{M_{w,N_2}\varepsilon_{bed}V_{bed}} - \frac{Q_0[N_2]}{V_{bed}} - \frac{[N_2] A dh}{V_{bed} dt}$
ICA	$\frac{d[ICA]}{dt} = \frac{F_{ICA}}{M_{w,ICA}\varepsilon_{bed}V_{bed}} - \frac{Q_0[ICA]}{V_{bed}} - \frac{[ICA] A dh}{V_{bed} dt}$
Potential catalyst sites S_p	$\frac{d[S_p]}{dt} = \frac{F_{cat}[S_{p,in}]}{\rho_{cat}(1 - \varepsilon_{bed})V_{bed}} - \frac{Q_0[S_p]}{V_{bed}} + R_{S_p} - \frac{[S_p] A dh}{V_{bed} dt}$
Y: $P_0, \lambda_0, \lambda_1, \lambda_2, \mu_0, \mu_1, \mu_2$	$\frac{d[Y]}{dt} = R_Y - \frac{Q_0[Y]}{V_{bed}} - \frac{[Y] A dh}{V_{bed} dt}$

The mass balance for the bed height is given by:

$$\frac{dh}{dt} = (R_{M_1}M_{w,1} + R_{M_2}M_{w,2}) \frac{V_{bed}}{\rho_p A} + \frac{F_{cat}^{in}/\rho_{cat}}{(1 - \varepsilon_{bed})A} - \frac{Q_0}{A} \quad (4)$$

And the steady state mass balance for the polymer in the bed is given by the following equation:^[40]

$$Q_0 = \frac{(R_{M_1}M_{w,1} + R_{M_2}M_{w,2})V_{bed}}{\rho_p} + \frac{F_{cat}^{in}/\rho_{cat}}{(1 - \varepsilon_{bed})} \quad (5)$$

where ρ_p and ρ_{cat} are the densities of the polymer (around 920 kg m⁻³) and catalyst (2800 kg m⁻³), respectively. The dimensions of the bed are given in Table 9.

Table 9. Reactor dimensions

Parameter	Designation	Value
D_{bed}	Bed diameter	4.75 m
ε_{bed}	Bed voidage	0.7
h	Height of the bed	13.3 m

2.4 Correlations of key properties

The main properties to be controlled in the gas-phase copolymerization of ethylene are the melt index (MI , or melt flow index MFI , g/10 min) and the polymer density (ρ_{pol}). Correlations are therefore needed to estimate these properties. The available correlations in the literature can be divided into two categories:

- A. Correlations which relate the final properties to the individual monomer conversions in the reactor (i.e. to reacted species) (Table 10).^[11] These correlations are universal and remain valid when varying the operating conditions.
- B. Correlations which relate the final properties to the operating conditions (i.e. T , P , or concentrations of unreacted species in the gas phase), such as ^[11]:

$$\ln MI_i = 3.5 \ln \left(k_0 + k_1 \frac{[M_2]}{[M_1]} + k_2 \frac{[M_3]}{[M_1]} + k_3 \frac{[H_2]}{[M_1]} \right) + k_4 \left(\frac{1}{T} - \frac{1}{T_0} \right) \quad (6)$$

$$\rho_i = \rho_0 + \rho_1 \ln MI_i - \left[\rho_2 \frac{[M_2]}{[M_1]} + \rho_3 \frac{[M_3]}{[M_1]} \right]^{\rho_4}$$

Where $k_{i(i=1-4)}$, $\rho_{k(k=0-4)}$ are tuning parameters and M_2 and M_3 are comonomers. Other correlations also exist in the open literature.^{[14] [41-44]} Such correlations are only valid for the set of operating conditions for which they were derived and cannot be used to account for thermodynamic effects such as the co-solubility effect. Therefore, such correlations are not valid during grade transition where the operating conditions change.

In this work, the correlations of the first category will be employed (Table 10), as only such correlations would be able to account for the co-solubility effect for instance. In this work, the correlations developed by McAuley and MacGregor^[11] for both MI and density are used (see Table 10).

The derivation of these correlations is based on physical interpretations. For instance, the melt index is highly correlated to the polymer molecular weight distribution and branching characteristics.^[45] To simplify, the instantaneous melt index is usually correlated to the instantaneous average polymer molecular weight M_w . The molecular weight is in turn affected by the concentration of monomer, comonomer and hydrogen. More particularly, hydrogen plays the role of a chain transfer agent in catalytic ethylene reactions, thus allowing to reduce the polymer molecular weight.^[46] It constitutes therefore a primary manipulated variable during grade transitions. The melt index considered in this work represents the flow rate of a molten polymer under the load of 2.16 kg at 190 °C (ASTM D1238).^[47,26]

Concerning the polymer density, it is strongly affected by the length and the number of short chain branches. Hence, it is mainly governed by the fraction of reacted comonomer in the copolymer (C_x) (Table 10).^[48] By creating short chain branches on the polymer, the comonomer allows reducing the polymer density. As a consequence the crystallinity of the polymer also

decreases.^[26] The comonomer constitutes the second important manipulated variable during grade transition. The correlation proposed by McAuley and MacGregor^[11] is based on patent data collected by Sinclair^[49], and it relates the instantaneous polymer density to the comonomer incorporation in the polymer by including C_x (where $C_x = \varphi_2 \times 100$, and $\varphi_2 = \frac{R_{M_2}}{R_{M_2} + R_{M_1}}$, see Table 5).

Table 10. Correlations of Category A for the properties of the polymer: MI (the same relation is used for instantaneous and cumulative properties) and density

Ref	Melt index (g/10 min)	Density (g cm ⁻³)	Data from
[11]	$M_w(\text{kg mol}^{-1}) = 111525 MI^{-0.288}$ (or $MI = 3.35 \times 10^{17} M_w^{-3.47}$)	$\rho_i = 0.966 - 0.02386 C_x^{0.514}$	Butene grades [49]
[50]	$MI = 2.7 \times 10^{19} M_w^{-3.92}$		[51]
[51,51]	$MI = 4.195 \times 10^{19} M_w^{-3.92}$		
[48]	$MI = 3 \times 10^{19} M_w^{-3.92}$	$\rho_i = -0.023 \ln C_x + 0.9192$	Octene grades [53]

The cumulative properties (of the polymer exiting the reactor) can be calculated from the instantaneous ones (those being produced at time t) by integration over the residence time (τ).

Therefore, the cumulative melt index (MI_c) becomes:^[54]

$$\frac{d(MI_c^{-0.286})}{dt} = \frac{1}{\tau} MI_i^{-0.286} - \frac{1}{\tau} MI_c^{-0.286} \quad (7)$$

Similarly, the cumulative density of the polymer (ρ_c) is given by: ^[8]

$$\frac{d(\rho_c^{-1})}{dt} = \frac{1}{\tau} \rho_i^{-1} - \frac{1}{\tau} \rho_c^{-1} \quad (8)$$

3. Grade transition strategy

Dynamic optimization is employed to optimize the transition between different grades of LLDPE in the FBR using the combined kinetic and thermodynamic model.

3.1 Formulation of the optimization problem

The manipulated variables are the flow rates of hydrogen and comonomer and the controlled outputs are the melt index and the polymer density.

The optimization problem can be written as follows:^[12]

$$\min_{\mathbf{u}(t)} J(\mathbf{u}(t), \mathbf{x}(t)), t \in [t_0, t_f] \quad (9)$$

$$\mathbf{u}_{\min} \leq \mathbf{u}(t) \leq \mathbf{u}_{\max} \quad (10)$$

where J is the objective function, $\mathbf{x}(t)$ is the vector of state variables (see Table 8) and $\mathbf{u}(t)$ represents the vector of manipulated variables, $\mathbf{u}(t) = [F_{H_2}, F_{com}]$. The inequality constraints (10) indicate the available ranges of manipulated variables.

3.2 Objective function

The considered objective function is the following:

$$J(\mathbf{u}) = \int_{t_0}^{t_f} w_1 \frac{|MI_i - MI_{sp}|}{MI_{sp}} + w_2 \frac{|MI_c - MI_{sp}|}{MI_{sp}} + w_3 \frac{|\rho_i - \rho_{sp}|}{\rho_{sp}} + w_4 \frac{|\rho_c - \rho_{sp}|}{\rho_{sp}} dt + w_5 \sum_{i=1}^2 \frac{\Delta u_i}{u_i(t_0)} \quad (11)$$

By considering both instantaneous and cumulative properties (of the melt index and polymer density), and by a good tuning the weighting factors w_i (with $i = 1 - 5$), one may accelerate the convergence of cumulative properties while keeping the instantaneous properties within an acceptable range. The last term on the right hand side of this equation is also intended to minimize the variation of the input during the transition, in order to avoid oscillations (as in model predictive control). The normalization of the different terms (i.e. the division by the set-points of the MI and density) allows for an easier tuning of the weighting factors. The indices i , c and sp refer to the instantaneous, cumulative and set-point properties, respectively.

At a constant reaction rate, the proposed objective function allows reducing the quantity of transition product as well as the transition time, even though the time is not explicitly minimized

in this function. If the reaction rate varies during the transition, then this objective function allows minimizing only the transition time. The minimization of the transition product would necessitate, in case of variable reaction rate, to multiply the criterion by the instantaneous reaction rate (R_p), as done by McAuley and MacGregor^[12] for instance. Takeda et al.^[13] suggested that the choice between minimizing the transition product and the transition time should be based on the market demand: where at high polymer sales and plant capacity production it is preferred to minimize the transition time; while at low polymer sales and reduced plant capacity it is preferred to minimize the transition production and authorize a longer transition time. A transition product can usually be sold, although at a discounted price.

3.2 Degrees of freedom of the inputs

It is usually sufficient to assume the manipulated variables (here, the flow rates of hydrogen and comonomer) to vary by a series of ramps during the transition.^[12] Based on the literature study and the residence time of the FBR (~4-6 hours in this study, depending on the operating conditions), the transition is divided into 5 intervals, where the final interval corresponds to the steady state interval, to maintain until the end of the production of the new grade. Thus, the optimization allows switching the flow rates every 2 hours during the first 8 hours, and the last ramp corresponds to the steady state flow rate of the new grade.

4. Simulation results and discussion

The proposed strategy is evaluated in grade transition starting from grade A, to grade B with higher or lower MI and ρ , then coming back to grade A, for both of the copolymerization systems (Table 11). These choices are based on LLDPE specifications, i.e. $MI \in [0.01-100]$ g/10min^[55] and $\rho \in [915-935]$ kg m⁻³^[56]. The duration of each grade production is usually defined by the market demand, the specifications or the claims of the production. Here, an arbitrary duration of production of each grade of 30 hours is implemented in both systems. No

particular change is required at the optimization level to change to shorter or longer production periods, only the final times need to be indicated. The initial steady state conditions, producing grade A, are given in

Table 12. This weighting factors were tuned as follows, except otherwise mentioned: $w_1 = 0.08$, $w_2 = 1$, $w_3 = 8$ $w_4 = 19$ and $w_5 = 10^4$. This choice was based on few simulation tests, in a way to ensure a compromise between fast convergence of the cumulative properties while reducing the overshoots of the instantaneous properties. Indeed, while allowing for big variations in the instantaneous properties leads to a faster convergence of the cumulative properties, some conditions of comonomer or hydrogen pressures might lead to polymer softening or sticking problems.^[3] In the following simulations, temperature control is assumed to be perfect in the bed, so that the working temperature is constant.

Table 11. LLDPE grades considered in the grade transition policy

Grade	Melt index Target (g / 10 min)		Density Target (kg m ⁻³)	
	1-hexene	1-butene	1-hexene	1-butene
A	0.54	4.5	923	918.5
B	2	2	916	922
A	0.54	4.5	923	918.5

Table 12. Initial conditions of the grade transition simulations (leading to grade A under steady state)

	1-hexene	1-butene
T (°C)	90	90
P_1 (bar)	9.4	7
P_2 (bar)	0.35	1.55
P_{ICA} (bar)	0.6	3.5
P_{H_2} (bar)	2.2	2.2

4.1 Copolymerization of ethylene and 1-hexene in presence of n-hexane as ICA

The optimization strategy was evaluated using the parameters of the first system, i.e. the copolymerization of ethylene with 1-hexene in presence of n-hexane. Note that the thermodynamic model was developed for this system for ethylene pressure of 10 bar and pseudo-component (i.e. comonomer plus ICA) pressure on the range of 0-1 bar. Therefore, the simulations (including the choices of the set-points) are conducted in a way to respect these ranges.

Figure 5 shows the results of the two grade transitions, from A to B, and from B back to A. This scenario was simulated using the following weighting factors: $w_1 = 0.08$, $w_2 = 1$, $w_3 = 8$, $w_4 = 19$ and $w_5 = 0$, therefore the instantaneous properties (MI_i and ρ_i) go beyond the set-point (SP) during the transition in order to accelerate the convergence of the cumulative properties (MI_c and ρ_c). This is related to the variations of the flow rates of hydrogen and 1-hexene, which are higher at the beginning of the grade transition and then they stabilize, as indicated by the increase in the pressure. The overshoots in the instantaneous properties can be reduced by reducing the weighting factors multiplying the cumulative properties w_2 and w_4 compared to those of the instantaneous properties w_1 and w_3 , or by considering $w_5 \neq 0$, or by adding constraints on the outputs, as discussed in the following scenarios. The MI is inversely proportional to the polymer molecular weight. Therefore, an increase in the hydrogen pressure during the transition, from grade A to B for instance, led to a decrease in the polymer molecular weight and thus to an increase in the melt index. Likewise, an increase in the comonomer pressure during the transition from grade A to B, led to an increase in the amount of short branches and thus to a decrease in the polymer density. The proposed strategy allows to move either to higher (grade A to grade B) or lower (B to A) values of MI , and vice versa for ρ .

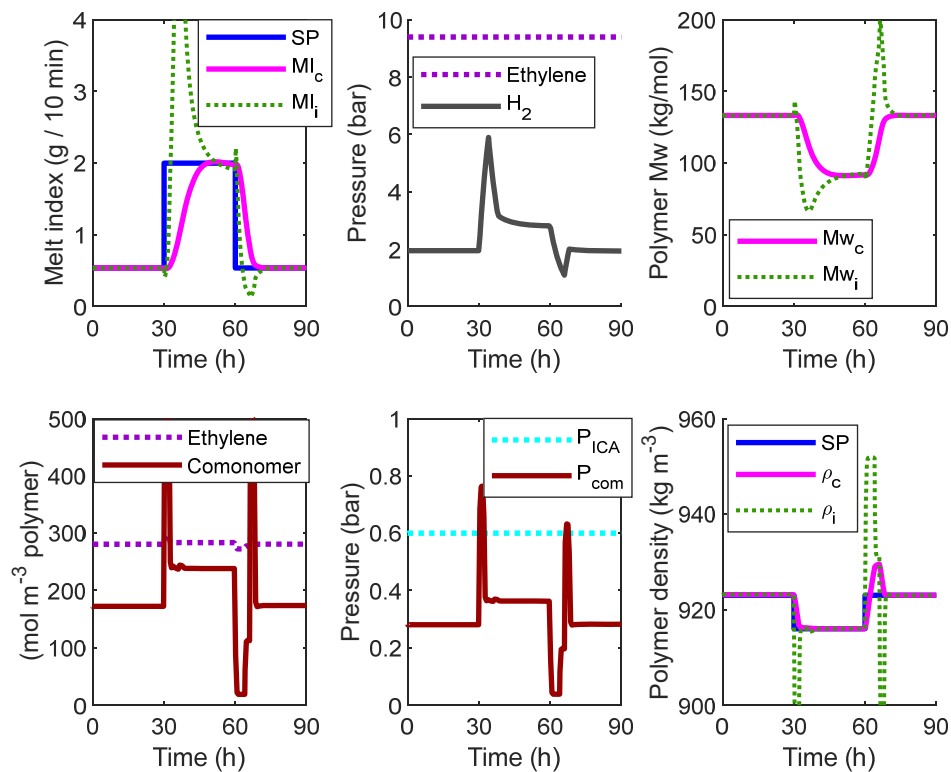


Figure 5. Grade transition in ethylene-1-hexene copolymerization in presence of n-hexane at 90°C ($w_1 = 0.08$, $w_2=1$; $w_3=8$, $w_4 = 19$, $w_5 = 0$).

The figure shows that the concentration of ethylene in the polymer particles (which constitutes the site of the reaction) does not change significantly during the transition, where the comonomer flow rate is varied, so the co-solubility effect is negligible in this sense and under the realized changes in the comonomer pressure. Note that the ethylene pressure is maintained constant in all the grades. However, the concentration of comonomer in the polymer particles is highly affected by these changes, which demonstrates the necessity of using a good thermodynamic model. The impact of the thermodynamic model is investigated more deeply in the last section. Note that the total pressure of comonomer and ICA reached 1.35 bar at the maximum in this simulation, but only for a short duration, and therefore the employed thermodynamic correlation remains valid during most of the time ($P_{ICA}+P_{com}=0-1$ bar).

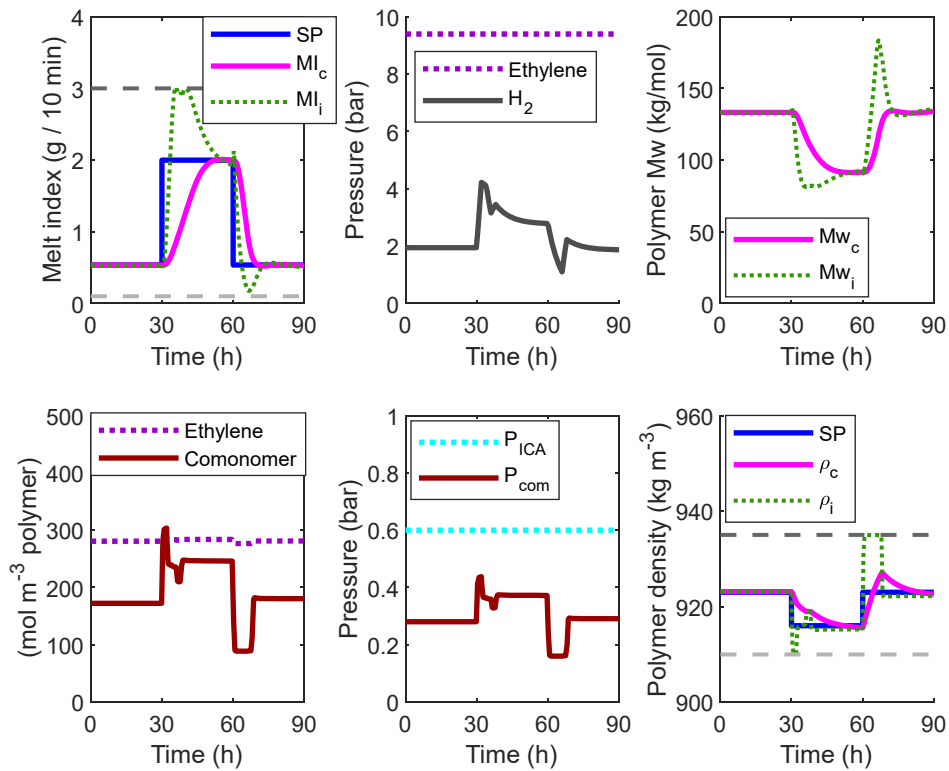


Figure 6. Grade transition in ethylene-1-hexene co-polymerization in presence of *n*-hexane: Tracking of the cumulative properties ($w_1=w_3=w_5=0$; $w_2=1$; $w_4=4$), with constraints on the instantaneous properties ($0.1 < MI_i < 3$ and $910 < \rho_i < 935$).

The same scenario presented in Figure 5 Figure 7. Grade transition in ethylene-1-butene co-polymerization in presence of iso-butane ($w_1 = 0.08$, $w_2=1$, $w_3=8$, $w_4 = 19$ and $w_5 = 0$). was simulated while tracking only the cumulative properties (i.e. $w_1=w_3=0$) and considering constraints on the instantaneous properties, as follows: $0.1 < MI_i < 3$ and $910 < \rho_i < 935$ (Figure 6). It can be seen that the convergence of the cumulative properties is slowed down compared to Figure 5, but the overshoots in the instantaneous properties (MI_i and ρ_i) are reduced and kept within the constraints. Adding hard constraints allows remaining within the acceptable range of properties, but it slows down the calculation. Another way to reduce the overshoots in the instantaneous properties, without considering constraints, consists of increasing the values of w_2 and w_4 with respect to w_1 and w_3 or by considering $w_5 \neq 0$.

4.2 Copolymerization of ethylene and 1-butene in presence of iso-butane as ICA

The proposed grade transition optimization strategy was evaluated in the second system: ethylene and 1-butene copolymerization in presence of iso-butane as ICA. Note that the thermodynamic model was developed for different conditions for this system: i.e. ethylene pressure of 7 bar and pseudo-component pressure on the range of 5-10 bars. The set-points of the melt index and polymer density of grades A and B were also set differently in this system, but still within LLDPE grades. The same weighting factors as the first system were considered.

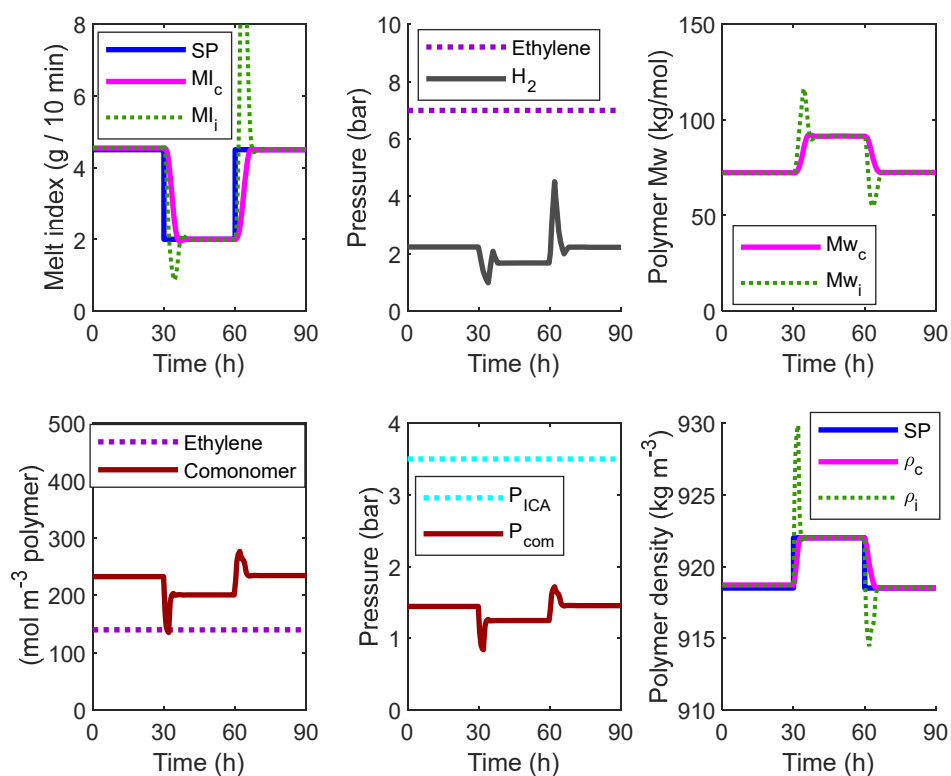


Figure 7. Grade transition in ethylene-1-butene co-polymerization in presence of iso-butane ($w_1 = 0.08$, $w_2=1$, $w_3=8$, $w_4 = 19$ and $w_5 = 0$).

Figure 7 shows the simulation results. The melt index converges in about 6 hours to the set-point, while the density converges to the set-point in 2 hours. The overshoots of the instantaneous properties remain acceptable, but they can be reduced by either manipulating the weighting coefficients (as discussed in the following scenario) or by adding hard constraints on

the outputs as discussed in the previous section. Note that the total pressure of comonomer and ICA is around 5 bar, therefore the employed thermodynamic correlation is valid ($P_{ICA}+P_{com}=5-10$ bar).

The last term of the objective function ($w_5 \sum_{i=1}^2 \frac{\Delta u_i}{u_i(t_0)}$) can allow minimizing the variation of the manipulated variables (flow rates of hydrogen and the comonomer), and thus to reduce the overshoots in the instantaneous properties. Indeed, injecting big amounts of hydrogen or comonomer rapidly increases the risk of polymer softening and stickiness.^[3] As a consequence, adding this term is expected to reduce the overshoots in instantaneous properties. Due to the low values of the variations of the flow rates, it was necessary to have a high weighting factor, $w_5 = 10^4$, to ensure an impact on the performance. Figure 8 shows the results when adding this term to the objective function, which is to be compared to Figure 7 done under the same conditions but without this term. The figure clearly shows that the pressures of hydrogen and comonomer undergo less changes. As a consequence, the instantaneous properties have lower overshoots. However, this delays a little the convergence of the cumulative properties to the set-points. A compromise is thus to be determined between fast convergence of the cumulative properties and less variation in the instantaneous properties.

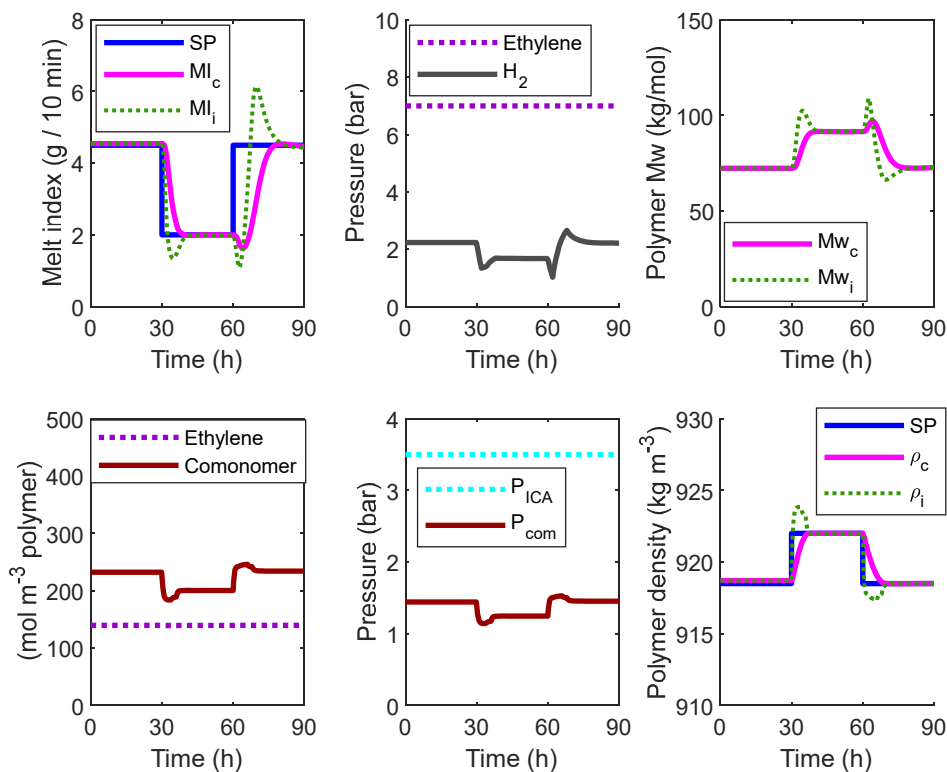


Figure 8. Grade transition in ethylene-1-butene: effect of the term $w_5 \sum_{i=1}^2 \frac{\Delta u_i}{u_i(t_0)}$ in the objective function ($w_1 = 0.08$, $w_2=1$, $w_3=8$, $w_4 = 19$ and $w_5 = 10^4$)

In order to evaluate the gain realized by the optimization strategy, its performance was compared to the case of injecting the optimal feed rates of the final grade during the transition (here called the final steady-state, SS), as done for instance by Rahimpour et al.^[8] (Figure 9). When employing a constant flow rate during the transition, the convergence time is that of the residence time of the reactor. It can be seen that employing the optimized varying flow rates during the transition allows to reduce the convergence times of the cumulative melt index and the density.

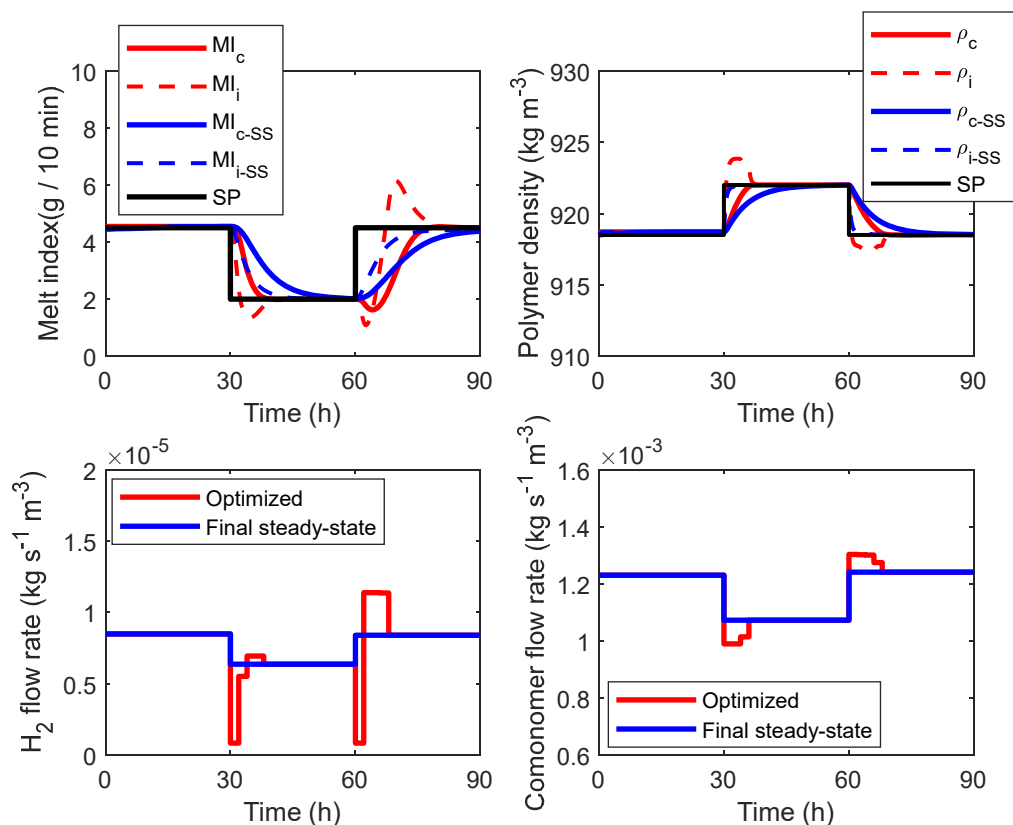


Figure 9. Grade transition in ethylene-1-butene copolymerization: comparison between the proposed grade transition strategy (leading to varying optimized flow rates during the transition) and injecting a constant flow rate during the transition (corresponding to the optimal flow rate of the final grade, under steady-state conditions)

4.3 Impact of the thermodynamic model

In order to demonstrate the importance of employing a good thermodynamic model in the optimization strategy, two scenarios were simulated. The first scenario was performed by assuming an error in the parameters of the thermodynamic model. The second system was used for this purpose, i.e. ethylene-1-butene co-polymerization in presence of iso-butane as ICA.

In Figure 10, an error is assumed in the parameters A and E in equations 1 and 2, related to the calculation of ethylene and comonomer concentrations in polymer, $[M_1^P]$ and $[M_2^P]$, respectively. It can be seen that the employed flow rates bring the process to different set-points than the desired ones (lower MI and ρ , as the used parameters A and E were assumed to be underestimated). Indeed, using lower A and E parameters in the model gives lower $[M_1^P]$ and

$[M_2^P]$ than the real ones. In order to correct ratios of monomer to hydrogen as well as to comonomer (to obtain the desired properties), the optimization strategy forces the decrease in the hydrogen flow rate, which leads to an increase in the polymer molecular weight, and a decrease in the MI . Similarly, the optimization forces the decrease in the comonomer flow rate, and as a result of errors in $[M_1^P]$ and $[M_2^P]$, a decrease in the polymer density is observed in this case). Note that the optimization strategy continues to work adequately, but as it is based on a wrong model it does not converge to the correct optimal points, therefore the use of an adequate thermodynamic model is essential.

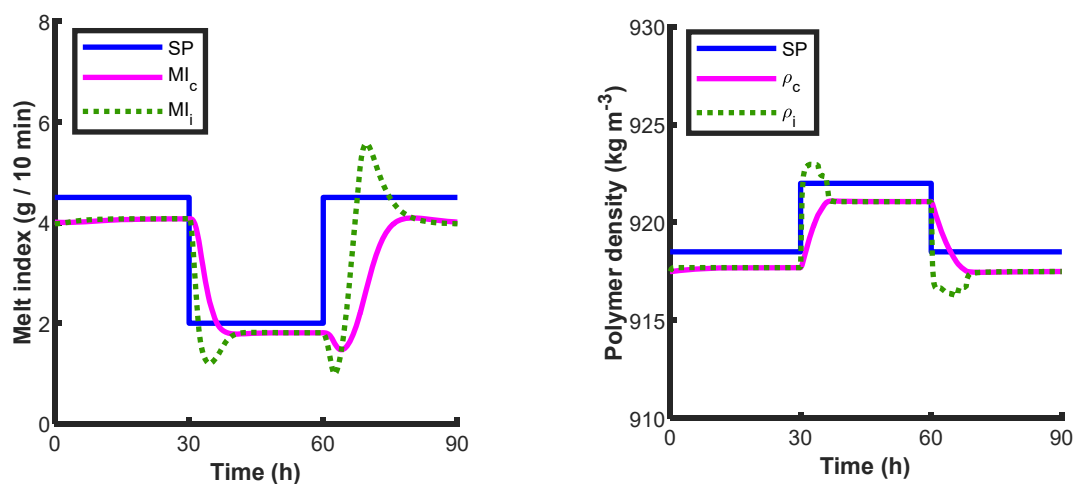


Figure 10. Influence of the thermodynamic model parameters on the process response, in ethylene and 1-butene copolymerization (Process parameters: $A = 1.98 \text{ mol m}^{-3} \text{ bar}^{-1}$, $E = 180 \text{ mol m}^{-3}$, Model parameters used for optimization: $A = 0.992 \text{ mol m}^{-3} \text{ bar}^{-1}$, $E = 90.2 \text{ mol m}^{-3}$)

The second scenario was performed by switching to a binary model to describe the solubility of the different species in the polymer (i.e. with no co-solubility effect). The system ethylene-1-hexene co-polymerization in presence of n-hexane as ICA was used for this simulation. In this case, the thermodynamic model leads to the calculation of an incorrect concentration of ethylene in the amorphous phase of the polymer, $[M_1^P] = 257 \text{ mol m}^{-3}$ at 10 bar ethylene and 90°C (as it assumes a binary system)^[27] instead of around 280 mol m^{-3} estimated in the pseudo-quaternary system. It also calculates an incorrect comonomer concentration in the polymer

particle $[M_2^P]$. The concentration of 1-hexene in a binary system (1-hexene+LLDPE)^[29] is expected to be higher compared to its concentration in a ternary system due to the anti-solvent effect of ethylene (as shown in Figure 2). However, combining ICA+comonomer in a pseudo-quaternary system leads to a global pressure which is much higher. As indicated by Figure 4, a small change in the pressure leads to a high change in the solubility of the pseudo-component, so the quaternary system leads to a much higher concentration of comonomer in the particles than in a binary system at the same pressure. Note however that the same flow rate is injected in the model and the process, but different reaction rates occur (due to the use of different thermodynamic models), therefore the comonomer pressure varies a lot between the two simulations, and therefore it is not straightforward to compare the concentration of comonomer in the model and the process in this simulation. In this simulation, when $[M_2^P]=165 \text{ mol m}^{-3}$ in the pseudo-quaternary system, it was $[M_2^P]=159 \text{ mol m}^{-3}$ in the binary model.

The simulation test was performed using the binary model for both the concentrations of ethylene and 1-hexene in the amorphous phase of the polymer (so the model and grade transition is simulated using the binary model while the process is simulated using the pseudo-quaternary model). Figure 11 shows that using a binary thermodynamic model and ignoring the co-solubility effect leads to a big drift of the properties from the set-points. Indeed, the model assumes a lower $[M_1^P]$ (so a lower polymer molecular weight and a higher *MI*). Therefore, the optimization strategy based on this model makes the decision to decrease the hydrogen flow rate. However, when implemented to the process (simulated using the pseudo-quaternary model, where the concentration of monomer is higher), this flow rate leads to a higher MW, so to a lower MI. Following the same reasoning, a drift in the polymer density occurs due to errors in both $[M_1^P]$ and $[M_2^P]$. This simulation demonstrates the importance of using an adequate thermodynamic model in the optimization strategy.

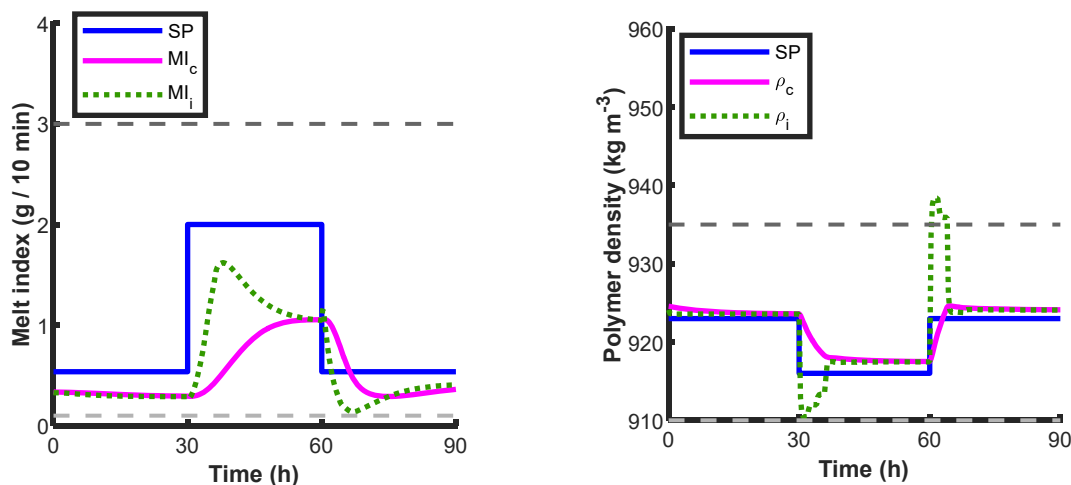


Figure 11. Influence of using binary thermodynamic model (not taking in account the co-solubility effect) on the process response. System ethylene-1-hexene copolymerization in presence of n-hexane at 90°C. ($w_1 = 0.08$, $w_2=1$, $w_3=8$, $w_4 = 19$ and $w_5 = 10^4$)

5. Conclusions

In this work, off-line dynamic optimization was implemented to optimize the grade transitions in a fluidized bed reactor of polyethylene. A combined kinetic and thermodynamic model was used in order to account for the co-solubility effects of the different gas species. The thermodynamic model is based on Sanchez-Lacombe EoS, but then simplified correlations were used to reduce the calculation time. Two copolymerizations were considered, the copolymerization of ethylene with 1-hexene in presence of n-hexane as ICA and the copolymerization of ethylene with 1-butene in presence of iso-butane. Some assumptions were made, mainly due to the lack of thermodynamic data in the literature, to allow the prediction of the solubility of the different species in PE in these quaternary systems.

The simulation results demonstrate the importance of the thermodynamic model in the optimization strategy. A good control of the polymer melt index and density could be realized by manipulating the flow rates of hydrogen and comonomer. Nevertheless, in both systems, the co-solubility effect of comonomer on ethylene was not observed, which is due to the low impact of the pseudo-component on the solubility of ethylene under the employed operating conditions

(pressure and temperature). The importance of the thermodynamic model was mainly related to evaluating the concentration of comonomer in the polymer during the transition, which highly impacts the polymer properties.

Both the instantaneous and the cumulative properties could be controlled, in a duration much lower than the residence time of the reactor. The role of the weighting factors, in the minimization function, is determinant at this level, where it can either give more importance to controlling the instantaneous properties (thus eliminating any overshoot) or on the contrary allow a faster control of the cumulative properties in detriment of the instantaneous ones. A compromise between these two options is necessary in order to ensure a fast convergence of the cumulative properties to the set-points (thus reduce the transition product) while avoiding big variations in the flow rates or pressures of hydrogen and comonomer as they may increase the risk of polymer sticking or softening. To reach the same objective, constraints on the instantaneous properties can be considered, but this slows down the calculation.

The proposed optimization tool should allow a more efficient operation and a better control of the polymer quality. The kinetic parameters and the correlations of the polymer properties used in this work were taken from literature, as well as the assumption of the bed to behave as a CSTR. These models can be replaced by more detailed models when available in the same optimization strategy. For instance, improvement at the level of the bed model can be done by considering a compartmental model and at the kinetic level by considering multiple site catalysts leading to bimodal molecular weight distributions and using correlations of the MI and polymer density adapted to such systems. Finally, the availability of more thermodynamic data or the use of a particle model accounting for diffusion would allow to improve the precision of the optimization strategy outcome.

Acknowledgements

This work was funded by Agence Nationale de la Recherche (Thermopoly project, grant N° ANR-16-CE93-0001-01). The authors would like to thank M. Robert Pelletier for his input on grade transitions in polymerization processes.

References

1. T. J. Hutley, M. Ouederni, *Polyolefins- the history and economic impact*, In: *Polyolefin Compounds and Materials*, Springer International Publishing Switzerland **2016**.
2. J. B. P. Soares, T. F. L. McKenna, *Polyolefin Reaction Engineering*, Wiley-VCH, Mannheim, Germany **2012**.
3. T. F. L. McKenna, *Macromol. React. Eng.* **2019**, 1800026.
4. J. M. J. III, R. L. Jones, T. M. Jones, S. Beret (Union Carbide Corp), *US Patent 4588790A*, **1986**.
5. A. Alizadeh, M. Namkajorn, E. Somsook, T. F. L. McKenna, *Macromol. Chem. Phys.* **2015**, 216, 903.
6. A. Alizadeh, M. Namkajorn, E. Somsook, T. F. L. McKenna, *Macromol. Chem. Phys.* **2015**, 216, 985.
7. J. A. Debling, G. C. Han, F. Kuijpers, J. Verburg, J. Zakka, W. H. Ray, *AIChE J.* **1994**, 40, 506.
8. M. R. Rahimpour, J. Fathikalajahi, B. Moghtaderi, A. N. Farahani, *Chem. Eng. Technol.* **2005**, 28, 831.
9. M. Ohshima, I. Hashimoto, T. Yoneyama, M. Takeda, F. Gotoh, in "Grade Transition Control for an Impact Copolymerization Reactor," *IFAC Proceedings*, Vol. 27, **1994**, 505.
10. H. Seki, M. Ogawa, S. Ooyama, K. Akamatsu, M. Ohshima, W. Yang, *Control Eng. Pract.* **2001**, 9, 819.

11. K. B. McAuley, *Ph.D. Thesis*, McMaster University, August, **1991**.
12. K. B. McAuley, J. F. MacGregor, *AIChE J.* **1992**, 38, 1564.
13. M. Takeda, W. H. Ray, *AIChE J.* **1999**, 45, 1776.
14. H.-S. Yi, J. H. Kim, C. Han, J. Lee, S.-S. Na, *Ind. & Eng. Chem. Res.* **2003**, 42, 91.
15. C. Chatzidoukas, J. D. Perkins, E. N. Pistikopoulos, C. Kiparissides, *Chem. Eng. Sci.* **2003**, 58, 3643.
16. R. H. Nyström, R. Franke, I. Harjunkoski, A. Kroll, *Comput. & Chem. Eng.* **2005**, 29, 2163.
17. D. Bonvin, L. Bodizs, B. Srinivasan, *Chem. Eng. Res. Des.* **2005**, 83, 692.
18. Y. Wang, H. Seki, S. Ohyama, K. Akamatsu, M. Ogawa, M. Ohshima, *Comput. & Chem. Eng.* **2000**, 24, 1555.
19. Y. Wang, G. S. Ostace, R. A. Majewski, L. T. Biegler, in "Optimal Grade Transitions in a Gas-phase Polymerization Fluidized Bed Reactor," *IFAC-PapersOnLine*, Vol. 52, **2019**, 448.
20. I. C. Sanchez, R. H. Lacombe, *Macromolecules* **1978**, 11, 1145.
21. R. Alves, M. A. Bashir, T. F. L. McKenna, *Ind. Eng. Chem. Res.* **2017**, 56, 13582.
22. P. A. Mueller, J. R. Richards, J. P. Congalidis, *Macromol. React. Eng.* **2011**, 5, 261.
23. A. Alizadeh, *Ph.D. Thesis*, Queen's University, July, **2014**.
24. A. S. Michaels, H. J. Bixler, *J. Polym. Sci.* **1961**, 50, 393.
25. M. A. Bashir, M. Al-haj Ali, V. Kanellopoulos, J. Seppälä, *Fluid Phase Equilib.* **2013**, 358, 83.
26. F. Nascimento de Andrade, *Ph.D. Thesis*, University Claude Bernard Lyon 1, February, **2019**.
27. W. Yao, X. Hu, Y. Yang, *J. Appl. Polym. Sci.* **2007**, 103, 1737.
28. H.-J. Jin, S. Kim, J.-S. Yoon, *J. Appl. Polym. Sci.* **2002**, 84, 1566.
29. A. Novak, M. Bobak, J. Kosek, B. J. Banaszak, D. Lo, T. Widya, W. Harmon Ray, J. J. de Pablo, *J. Appl. Polym. Sci.* **2006**, 100, 1124.

30. M. A. Bashir, V. Monteil, V. Kanellopoulos, M. A.-H. Ali, T. McKenna, *Macromol. Chem. Phys.* **2015**, *216*, 2129.
31. W. Yao, X. Hu, Y. Yang, *J. Appl. Polym. Sci.* **2007**, *104*, 3654.
32. W. M. R. Parrish, *J. Appl. Polym. Sci.* **1981**, *26*, 2279.
33. S. J. Moore, S. E. Wanke, *Chem. Eng. Sci.* **2001**, *56*, 4121.
34. A. B. de Carvalho, P. E. Gloor, A. E. Hamielec, *Polymer* **1989**, *30*, 280.
35. K. B. McAuley, J. F. MacGregor, A. E. Hamielec, *AIChE J.* **1990**, *36*, 837.
36. J. Sun, H. Wang, M. Chen, J. Ye, B. Jiang, J. Wang, Y. Yang, C. Ren, *J. Appl. Polym. Sci.* **2017**, *134*.
37. N. M. Ghasem, W. L. Ang, M. A. Hussain, *Korean J. Chem. Eng.* **2009**, *26*, 603.
38. S. Chakravarti, W. H. Ray, *J. Appl. Polym. Sci.* **2001**, *80*, 1096.
39. A. Alizadeh, T. F. L. McKenna, *Macromol. Symp.* **2013**, *333*, 242.
40. H. Hatzantonis, H. Yiannoulakis, A. Yiagopoulos, C. Kiparissides, *Chem. Eng. Sci.* **2000**, *55*, 3237.
41. P.-O. Larsson, J. Akesson, N. Andersson, in "Cost Function design for Economically Optimal Grade Changes for a Polyethylene Gas Phase Reactor," Proceeding of the 50th IEEE CDC-ECC, Orlando, FL, USA (December, **2011**).
42. M. Ogawa, M. Ohshima, K. Morinaga, F. Watanabe, *J. Process Control* **1999**, *9*, 51.
43. A. Gisas, B. Srinivasan, D. Bonvin, *Comput. Aided Chem. Eng.* **2003**, *15*, 463.
44. A. Kiashemshaki, N. Mostoufi, R. Sotudeh-Gharebagh, S. Pourmahdian, *Chem. Eng. Technol.* **2004**, *27*, 1227.
45. M. S. Abbas-Abadi, M. N. Haghghi, H. Yeganeh, *J. Appl. Polym. Sci.* **2012**, *126*, 1739.
46. V. Touloupides, V. Kanellopoulos, P. Pladis, C. Kiparissides, D. Mignon, P. Van-Grambezen, *Chem. Eng. Sci.* **2010**, *65*, 3208.
47. M. F. Bergstra, G. Weickert, G. B. Meier, *Macromol. React. Eng.* **2009**, *3*, 433.

48. J. Shi, L. T. Biegler, I. Hamdan, *AIChE J.* **2016**, *62*, 1126.
49. K. B. Sinclair, *Process Economics Report*, SRI International, Menlo Park, CA **1983**.
50. K. C. Seavey, Y. A. Liu, N. P. Khare, T. Bremner, C.-C. Chen, *Ind. & Eng. Chem. Res.* **2003**, *42*, 5354.
51. T. Bremner, A. Rudin, D. G. Cook, *J. Appl. Polym. Sci.* **1990**, *41*, 1617.
52. M. Embiruçu, D. M. Prata, E. L. Lima, J. C. Pinto, *Macromol. React. Eng.* **2008**, *2*, 142.
53. A. J. Peacock, *Handbook of polyethylene: structures: properties, and applications*, CRC Press, USA **2000**.
54. E. H. Lee, T. Y. Kim, Y. K. Yeo, *Korean J. Chem. Eng.* **2008**, *25*, 613.
55. C. Chatzidoukas, *Ph.D. Thesis*, University of London, **2004**.
56. D. P. Lo, W. H. Ray, *Ind. Eng. Chem. Res.* **2006**, *45*, 993.
57. H.-S. Yi, J. H. Kim, C. Han, J. Lee, S.-S. Na, *Ind. Eng. Chem. Res.* **2003**, *42*, 91.